CrystEngComm

Additive Controlled Packing Polymorphism in Series of Halogen Substituted Dithieno[3,2-a:2',3'-c]phenazines

Journal:	*CrystEngComm*
Manuscript ID	CE-ART-04-2023-000387.R1
Article Type:	Paper
Date Submitted by the Author:	30-May-2023
Complete List of Authors:	Timofeeva, Tatiana; New Mexico Highlands University, Biology & Chemistry Averkiev, Boris; University of Minnesota, Chemistry Castaneda, Raul; New Mexico Highlands University Fonari, Marina; Institute of Applied Physics, ; Institute of Applied Physics, Jucov, Evhgeni; New Mexico Highlands University

Additive Controlled Packing Polymorphism in Series of Halogen Substituted Dithieno[3,2-*a*:2',3'-*c*]phenazines

Boris B. Averkiev,[a] Raúl Castañeda,[b] Marina S. Fonari,[b,c] Evgheni V. Jucov,[b] and Tatiana V. Timofeeva[b]*

[a]*Department of Chemistry, Kansas State University, Manhattan, KS 66506, United States*

[b]*Department of Chemistry, New Mexico Highlands University, Las Vegas, NM 87701, United States*

E-mail: **tvtimofeeva@nmhu.edu**

[c]*Institute of Applied Physics, Moldova State University, Academiei str, 5 MD2028, Chisinau Republic of Moldova*

ABSTRACT: For a series of substituted dithieno[3,2-*a*:2',3'-*c*]phenazine derivatives X-ray diffraction studies have been carried out. It was found that in dependence on crystallization conditions (solution or gas phase and additives) several packing polymorphs for phenazine derivatives with H, F and Cl substituents were obtained. For F-substituted compound an unusual number of symmetrically independent molecules (six and four) were found among its crystalline polymorphs. Comparison of the calculated lattice energies revealed insignificant energy differences between the polymorphs, thus explaining the existence of the large number of polymorphs in this series of materials. TD-DFT calculations of HOMO-LUMO gap for these molecules demonstrated close correspondence to the results of the previously published electrochemical measurements.

Keywords: Dithieno[3,2-*a*:2',3'-*c*]phenazine / polymorphism / single crystals / high Z' structures / X-ray diffraction

1. INTRODUCTION

Multiple sources tell that in spite of significant efforts invested in studies of polymorphism of molecular crystals, it is still almost impossible to theoretically predict the structure of thermodynamically stable polymorph from the variety of possible crystalline forms for a particular material and to figure out how to obtain certain polymorph. Therefore, the famous quotation from McCrone that "the number of forms known for a given compound is proportional to the time and money spent in research on that compound" [1] is still in place and has many supporters[2-5]. It is interesting to mention, however, that for many materials a second polymorph was never found, most probably because researchers, after establishing structure of material under study did not attempt detailed study of material polymorphism. On the other hand, in many cases the second polymorph modification was found long after the first one, and was discovered quite unexpectedly when, for instance, the materials under investigation have been crystallized in presence of another compound. For example, crystals of maleic acid were characterized as early as 1881 and until 2006, for 124 years, has considered to be monomorphic[6]. However, the attempt to co-crystallize this acid with caffeine brought to discovery the second form of maleic acid[4]. The appearance of maleic acid form II should serve as a precaution against assuming that consistent production of only one crystal form rules out the appearance of new polymorphs. It was suggested that the presence of an additive (coformer) may have played a structure directing role in the growth of this latent crystal form[4]. A similar situation was observed for sym-trinitrobenzene where two new stable crystal forms of the 120-year-old compound were obtained by applying an additive, trisindane, and changing thermodynamic conditions of crystal growth[7]. Other polymorphs may be discovered during exploration of new solvent/co-solute combinations[4]. This statement is supported by the examples of co-crystallization which enable formation of new polymorphs. For instance, induced conformational polymorphism of 1,1-dicyano-2-(4-hydroxy-3-methoxyphenyl)-ethene was observed during attempts to grow its co-crystals with L-proline and L-tartaric acid[8]. Co-crystallization of 8-hydroxyquinoline with acetaminophen resulted in a new monoclinic packing polymorph of 8-hydroxyquinoline[9]. This effect was discussed in a more general way as additive-induced polymorphism or additive controlled crystallization in several reviews[10-12]. The weak interactions such as hydrogen bonding, halogen bonding and other dispersive interactions are the reliable and widely used tools that play crucial role in self-assembly and molecular recognition in the solid-state.[13,14]

Polymorphism is especially important for crystal engineering of organic π-conjugated materials, which demonstrate specific intermolecular interactions, including stacking interactions and every polymorph has specific physical properties useful or preventing their use for organic electronic technology. Molecules in such materials can be arranged in layers or in stacks and different arrangement can alternate physical properties of these materials including their electronic properties.[15-17]

Recent findings demonstrate the achievements in control of polymorphism aimed to show that so far polymorphism can be considered not as a drawback, but more as an opportunity that allows to control and fully exploit the intrinsic properties of polymorphism and transitions between its various metastable states, through fine-tuning of molecular packing in a reproducible manner.[18-20]

Introducing various substituents, such as halogen atoms or bulky groups, allow modulation of intermolecular interactions, and molecular packing, making some crystal structures preferable in terms of their properties.[21]

One such property is charge transport in organic semiconductors which can be altered dramatically in various polymorphs of the same compound due to variation of intermolecular interactions.[22] Though some features of molecular arrangement and intermolecular interactions in the charge transfer crystalline polymorphs have been discussed, there is no general approach that can predict these properties based on crystal structure. Accumulation of experimental data will help to move closer to formulation of such approach. The influence of weak intermolecular interactions on electronic properties in crystalline polymorphs of molecular compounds was studied experimentally and theoretically.[23-30] Two polymorphs of fluorinated 5,11-bis(triethylsilylethynyl)anthradithiophene with slightly different packing show different temperature dependence of the charge mobilities.[23] From the two polymorphs of thieno[3,2-b]thiophenethiazolo[5,4-d]thiazole, only a herringbone packed polymorph with continuous π–π stacking and S···S close contacts displayed p-type semiconductive properties, while the polymorph with slipped-stacked packing, in which molecules are arranged in isolated groups of tetramers, is an insulator.[26] For these polymorphs, calculations suggest the possibility of n-type character of conductivity, which was not observed in the experiments. The theoretical calculations of the charge transport properties for three crystalline polymorphs of 9,10-bis((E)-2-(pyrid-2-

yl)vinyl)anthracene have shown that the different character of molecular overlapping and intermolecular interactions affect the transfer integrals and reorganization energy in these three polymorphs.[27] The calculations using density-functional theory and Marcus charge transport theory revealed that different intermolecular interactions in four quinacridone polymorphs impact their hole mobility.[28] All four of them can be used as electron transport materials, but only α^{II} polymorph can be used as dipolar transport material. The influence of the weak interactions such as hydrogen bonding and π…π interactions on charge transport in various organic polymorphs was also studied theoretically, where correlations between charge transfer degree and week intermolecular interactions in polymorph crystals (H-bonds, stacking) was established.[29]

Reported in this publication dithienophenazines (Scheme 1), represent a wide class of novel organic π-conjugated compounds, with the same core structure as shown in Scheme 1, but various positions of heteroatoms.[31-39] These compounds attracted considerable interest as potential materials for diverse applications in organic electronics, such as organic light-emitting diodes (OLED),[31] as well as pendant groups in donor-acceptor polymers for solar cell application[32-34] in dye-sensitized solar cells,[35-37] and in anion probe.[38] This aromatic system with sp^2-hybridized nitrogen atoms might be capable in formation of C–H···N hydrogen bonds, and those had been shown to assist molecular self-assembly and increase charge mobility in the thin films.[39] Surprisingly, according to Cambridge Structural Database, only few crystal structures of compounds with the same core and same positions of heteroatoms as presented in Figure 1 were reported. The initial goal of this project was creation of dithienophenazines cocrystals with acceptor molecules, for instance, tetracyanoquinodimethane to obtain charge transfer materials. Unfortunately, our attempts allowed to obtain only one cocrystalline material. Structure of the charge-transfer cocrystal of dithieno[3,2-a:2',3'-c]phenazine DTPhz, (X=H, R=H) with TCNQ was described earlier in.[40] Nonetheless, these attempts brought to formation of three groups of polymorphs. It should be mentioned also that in[41] synthesis, structure and mechanooptics of pure (DTPhz, X=H, R=H) were presented. Obtained 1D crystals revealed very uncommon properties such as elastic bending in combination with efficient transmission of optical signals of different colors that suggest potential use of such material for crystalline flexible waveguides. A series of DTPhz derivatives with R = Hal, and X=C_nH_{2n+1} was presented.[42, 43] Their structures were modified

with halogen substituents and linear alkyl chains of various lengths, and they were used as building blocks to assemble luminescent one-dimensional nano/microcrystals.

In the presented paper, molecular and crystal structures in series of halogen and trimethylsilyl (TMS) substituted dithieno[3,2-a:2',3'-c]phenazines (Scheme 1) and their polymorphism are considered on the base of the experimental diffraction data.

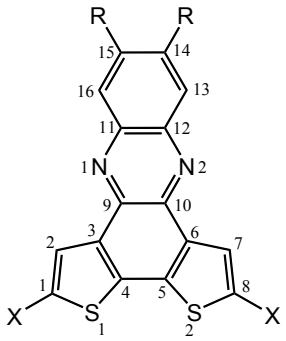

Scheme 1. The structural formula of studied DTPhz derivatives with atoms numbering scheme; R=H, F, Cl, Br; X=H, TMS.

In addition to experimental structures, the theoretical calculations of single molecules and crystal structures were carried out to analyze the electronic characteristics of the molecules, in particular, their HOMO-LUMO gaps and excitation energies. For R-DTPhz derivatives (R=H, F, Cl, Br), the quantum chemical and force field calculations of crystal structures were carried out for both, experimentally studied polymorphs, and for some hypothetical polymorphs to investigate the possibility to obtain other polymorphs of these compounds.

Development of a concise multi-gram approach to 2,7-bis(trimethylsilyl)benzo[2,1-*b*:3,4-*b*']dithiophene-4,5-dione (**TMS-BDDO**) previously allowed for preparation of a series 2,7-dihalo-BDDO derivatives, which were used to investigate the influence of the halide substituents as well as crystallization conditions on their molecular packing in crystals.[44-47] In perspective, it would be possible to cocrystallize presented here donor molecules with acceptor molecules to engineer charge transfer (CT) materials in form of cocrystals and thin films.[40, 41]

2. MATERIALS AND METHODS

Synthesis of materials. Key starting material for the preparation of dithieno[3,2-*a*:2',3'-*c*]phenazine derivatives, **TMS–BDDO**, was prepared in two steps from commercially available 2-bromothiophene.[45-47] Dithieno[3,2-*a*:2',3'-*c*]phenazine derivatives **H–DTPHz**, **F–DTPHz** and **Cl–DTPHz** were prepared in two steps by the condensation reaction **TMS–BDDO** with benzene-1,2-diamine derivatives followed by the removal of trimethylsilyl (TMS) groups with

tetrabutylammonium fluoride. Detailed descriptions of these procedures are given in.[40] **Br–DTPHz** derivative was prepared from the unsubstituted **BDDO** by condensation with 4,5-dibromobenzene-1,2-diamine.

Growth of single crystals for X-ray analysis

Crystal growth for X-ray diffraction studies was carried out from solution and from vapor phase. Usually, several solvents were used for materials crystallization. Crystallization from dichloromethane (DCM) resulted in needle-shaped yellow **α H–DTPhz** and **α F–DTPhz** crystals. The second polymorphs, yellow prism **β H–DTPhz**, and yellow plate **β F-DTPhz**, were obtained via physical vapor transport (PVT) during attempts to cocrystallize them with TCNQ using this method.[48] The third polymorph, yellow needles of **γ F–DTPhz,** was obtained during attempt to cocrystallize it with TCNQ from dichloromethane solution. The yellow needles of **α Cl–DTPhz** were crystallized from chloroform solution, and orange blocks of **β Cl–DTPhz** were crystallized from 1:1 mixture of toluene and DCM. The orange blocks of **Br–DTPhz** were crystallized from toluene solution. **TMS-F-DTPhz** and **TMS-Cl-DTPhz** were crystallized from chloroform solution.

Single-Crystal X-ray Diffraction. Single-crystal experiments were carried out with Bruker SMART diffractometer equipped with an APEX II CCD detector using MoKα (λ = 0.71073 Å) radiation. All single crystal diffraction data were integrated using the SAINT software program within the APEX II software suite and absorption corrections were applied using SADABS.[49, 50] The TWINABS program was used for **γ F–DTPhz** crystals, which were non-merohedral twins.[51] The structures were solved and refined using SHELXTL programs.[52 53] All non-hydrogen atoms were located in difference Fourier maps and were refined anisotropically. Hydrogen atoms were added geometrically and refined with the use of a riding model. Crystal data, data collection and structure refinement details are summarized in Tables 1 and 2. The shortest intermolecular contacts as calculated by Mercury [54] are summarized in Table S1. The Hirshfeld surface analysis and distribution of types of intermolecular interactions within polymorphic series and between structures was carried out using CrystalExplorer17 software[55] and results are summarized in Supporting Information (Figs. S1-S16, Table S2)

CCDC 1576235–1576244 contains the supplementary crystallographic data for this paper. These data can be obtained free of charge from The Cambridge Crystallographic Data Centre (CCDC) via www.ccdc.cam.ac.uk/structures.

Table 1. Selected crystallographic data for R-DTPhz (R=H, F, Cl, Br) derivatives

	α H-DTPhz	**β H-DTPhz**	**α F-DTPhz**	**β F-DTPhz**	**γ F-DTPhz**	**α Cl-DTPhz**	**β Cl-DTPhz**	**Br-DTPhz**
Empirical formula	$C_{16}H_8N_2S_2$	$C_{16}H_8N_2S_2$	$C_{16}H_6F_2N_2S_2$	$C_{16}H_6F_2N_2S_2$	$C_{16}H_6F_2N_2S_2$	$C_{16}H_6Cl_2N_2S_2$	$C_{16}H_6Cl_2N_2S_2$	$C_{16}H_6Br_2N_2S_2$
Method, solvent, additive	Solution dichloromethane	PVT, TCNQ	Solution dichloromethane	PVT, TCNQ	Solution, dichloromethane, TCNQ	Solution, chloroform	Solution, toluene /DCM	Solution, toluene
Color	yellowish	yellow	yellowish	yellow	yellow	yellow	light-orange	orange
FW	292.36	292.36	328.35	328.35	328.35	361.25	361.25	450.17
Crystal System	Orthorhombic	Triclinic	Triclinic	Triclinic	Monoclinic	Monoclinic	Orthorhombic	Orthorhombic
Space Group	$P2_12_12_1$	P-1	P-1	P-1	$C2/c$	$P2_1/n$	$P2_12_12_1$	$P2_12_12_1$
a, Å	4.8175(7)	8.317 (1)	13.536(2)	14.175(4)	26.70(2)	4.9687(7)	9.076(1)	9.034(2)
b, Å	15.993(2)	10.874 (2)	15.446(2)	14.277(4)	4.815(3)	18.077(3)	10.183(1)	10.366(2)
c, Å	16.143(2)	14.978(2)	19.582(2)	16.501(4)	20.82(2)	15.442(2)	29.957(4)	30.468(6)
α, °	90	99.580(2)	80.141(2)	112.680(3)	90	90	90	90
β, °	90	102.642(2)	84.184(2)	95.238(3)	104.90(1)	92.142(2)	90	90
γ, °	90	101.257(2)	78.220(2)	115.518(3)	90	90	90	90
V_{calc}, Å^3	1243.7(3)	1265.0(3)	3939.3(8)	2644(1)	2586(3)	1386.0(4)	2768.7(6)	2853(1)
Z	4	4	12	8	8	4	8	8
Z’	1	2	6	4	1	1	2	2
ρ_{calc}, g/cm^3	1.561	1.535	1.661	1.649	1.687	1.731	1.733	2.096
T, K	100	215	100	215	215	100	215	100
μ^{-1}, mm	0.416	0.409	0.425	0.422	0.431	0.764	0.765	5.970
Unique reflections	3622	8105	20489	17407	3758	4257	8042	8357
Unique reflections with $I > 2\sigma(I)$	3354	6740	17353	12125	2488	3615	7941	7595
R_{int}	0.0485	0.0277	0.0325	0.0404	–	0.0274	0.0188	0.0660
R_1 ($I > 2\sigma(I)$)	0.0324	0.0398	0.0608	0.0439	0.0564	0.0325	0.0268	0.0346
wR_2 ($I > 2\sigma(I)$)	0.0718	0.1033	0.1499	0.1042	0.1193	0.0783	0.0685	0.0841

Table 2. Selected crystallographic data for TMS-DTPhz derivatives

	TMS-F-DTPhz	**TMS-Cl-DTPhz**
Empirical formula	$C_{22}H_{22}F_2N_2S_2Si_2$	$C_{22}H_{22}Cl_2N_2S_2Si_2$
Method, solvent	Solution, chloroform	Solution, chloroform
Color	yellow	yellow
FW	472.71	505.61
Crystal System	Orthorhombic	Triclinic
Space Group	*Pnma*	*P*-1
a, Å	26.626(4)	7.3053(19)

b, Å	6.9557(11)	10.911(3)
c, Å	12.568(2)	15.153(4)
α, °	90	88.935(4)
β, °	90	85.183(4)
γ, °	90	82.192(4)
V_{calc}, Å^3	2327.6(6)	1192.4(5)
Z	4	2
Z'	0.5	1
ρ_{calc}, g/cm^3	1.349	1.408
T, K	215	100
μ^{-1}, mm	0.360	0.561
Unique reflections	3666	5707
Unique reflections with $I > 2\sigma(I)$	2853	4419
R_{int}	0.0569	0.0298
R_1 ($I > 2\sigma(I)$)	0.0459	0.0452
wR_2 ($I > 2\sigma(I)$)	0.0640	0.0658

Theoretical calculations. Quantum chemical calculations of molecular geometry, HOMO and LUMO energy levels, and excitation energies (TD-DFT method) for DTPhz derivatives were carried out at the B3LYP/6-311G(d) and M06/6-311G(d) levels of theory using the GAUSSIAN09 program.[56] The initial molecular coordinates were taken from crystallographic data.

The geometries and energies of crystal structures of R-DTPhz polymorphs were calculated using empirical force field and quantum chemical approaches. Force field calculations were done with COMPASS force field implemented in Cerius2 software.[57,58] Quantum chemical calculations were done with Perdew-Burke-Ernzerhof functional with the addition of a semi-empirical Grimme correction (PBE-D method) and ultra-soft pseudopotentials (PBE-RRKJUS for C, N, H, and PBE-N-RRKJUS_PSL for S, F Cl, Br atoms) implemented in version 5.0.1 of Quantum Espresso program.[59-62] The initial geometries were taken from the experimental X-ray crystal structures. The full optimization of the unit cell parameters along with all atomic positions was carried out.

]

3. RESULTS AND DISCUSSION

Molecular Structure. X-ray analysis revealed that the molecules of **R–DTPhz** (R = H, F, Cl, Br) are planar with mean least square deviation for aromatic core ranging from 0.01 up to 0.06 Å. All molecules possess the local C_{2v} symmetry. The molecular geometries of dithiophene fragment

are similar to geometries of this fragment in 52 structures from the Cambridge Structural Database (CSD, Version 5.43 of November 2022).[63] All four S–C bonds are essentially the same (1.719(2) – 1.728(2) Å) and comparable with average values from CSD 1.725(10) and 1.732(15) Å for S(1)–C(4) (equivalent to S(2)–C(5)) and S1–C1 (equivalent to S(2)–C(8)), respectively. The molecular geometries of phenazine core are similar to geometries of this fragment in 348 structures from CSD. For all molecules, the C(9)-C(10) (1.438(4) – 1.457(4) Å) bond distances (Scheme 1) are elongated in comparison to C(11)–C(12) bond (1.415(4) – 1.441(4) Å) and average CSD value 1.432 (13) Å due to conjugation with dithiophene fragment. The N(1)–C(9) and N(2)–C(10) bonds (1.328(3) – 1.340(3) Å) are slightly shortened in comparison to average value from CSD 1.344(12) Å, while N(1)–C(11) and N(2)–C(12) bonds (1.343(3) – 1.357(3) Å) are slightly elongated. There is also possible to observe bond length alternation in the six-membered ring C(11)-C(16): bonds C(13)–C(14) and C(15)–C(16), 1.36 Å, are shorter than four other bonds, equal to 1.42 Å. Such experimentally found bond length distribution corresponds to Scheme 1. The halogen substituents in the **F-DTPhz**, **Cl-DTPhz**, and **Br-DTPhz** molecules do not alter their geometries significantly. Bond lengths in these structures are similar to the corresponding values in **H–DTPhz**.

In addition to X-ray experiments, the quantum-chemical calculations (B3LYP/6-311G(d) and M06/6-311G(d)) of these molecules in gas phase have been carried out. The calculated molecular geometries are in good agreement with the experimental results. The mean-unsigned errors for B3LYP/6-311G(d) and M06/6-311G(d) methods are 0.007 and 0.008 Å, respectively. The largest disagreements were observed for C–S bonds. The calculated S(1)–C(4) bond lengths (X-ray average 1.722 Å) are 1.731 and 1.741 Å for M06 and B3LYP functionals, respectively. The S(1)–C(1) bond lengths (X-ray average 1.725 Å) are 1.738 and 1.746 Å.

For molecules with TMS substituents, **TMS-F-DTPhz**, and **TMS-Cl-DTPhz**, the S(1)–C(1) and S(2)–C(8) bonds, adjacent to TMS, are slightly elongated in comparison to S(1)–C(4) and S(2)–C(5) bonds. This observation is in agreement with quantum-chemical calculations of these molecules. The aromatic systems in both molecules are planar.

Molecular Packing in Crystals. In spite of similar molecular shapes, in crystals of studied compounds, molecules packed differently demonstrating for three of materials the so-called packing polymorphs. So, seven packing motifs were observed for **R-DTPhz** (R = H, F, Cl, Br) compounds.

For **H-DTPhz**, two polymorphs with very distinctive crystal packings were obtained by crystallization from solution (orthorhombic) and from vapor phase (triclinic). The orthorhombic **α H-DTPhz** polymorph contains one crystallographically unique molecule. The molecules are packed in stacks along [1 0 0] direction (Figure 1a). Each stack contains identical molecules related by translation (Figure 2) with the interplanar distance equal to 3.38 Å. Of other specific interactions only weak edge-to-edge CH···N contacts between neighboring stacks were found. The molecules from neighboring stacks related by the two-fold screw axis form the interplanar angle of 65.72 ° and are interconnected by weak CH···N hydrogen bonds [C(13)-H(13)···N2, 3.486(3), 2.73 Å; ∠CHN 137.6 °, and C(8)-H(8)···N1, 3.340(3), 2.53 Å; ∠CHN 143.4 °, Table S1].

The triclinic **β H–DTPhz** polymorph (Figure 1b) contains two crystallographically unique molecules, **A** and **B** located almost in perpendicular planes. Molecules **A** are arranged in the centrosymmetric stacking dimers (Figure 3a) with big overlapping area and interplanar distance 3.53 Å. The dimers are stacked in the [1 0 0] direction. Molecules **B** only slightly overlap (Figure 3b) with interplanar distance of 3.46 Å, and they do not form stacks. On the other hand, the shortened intermolecular S(1B)…S(2B) contacts of 3.4857(7) Å were registered between adjacent **B** molecules. These contacts link molecules in planar centrosymmetric dimers that are further interlinked in the planar tapes through the stabilizing H…H contacts, H(13B)···H(14B)=2.158 Å (Table S1), [64new] both types of interactions are absent in **α H-DTPhz**. It should be mentioned that in α form molecules are packed in parallel manner, which is different from β modification where they are packed in an anti-parallel manner.

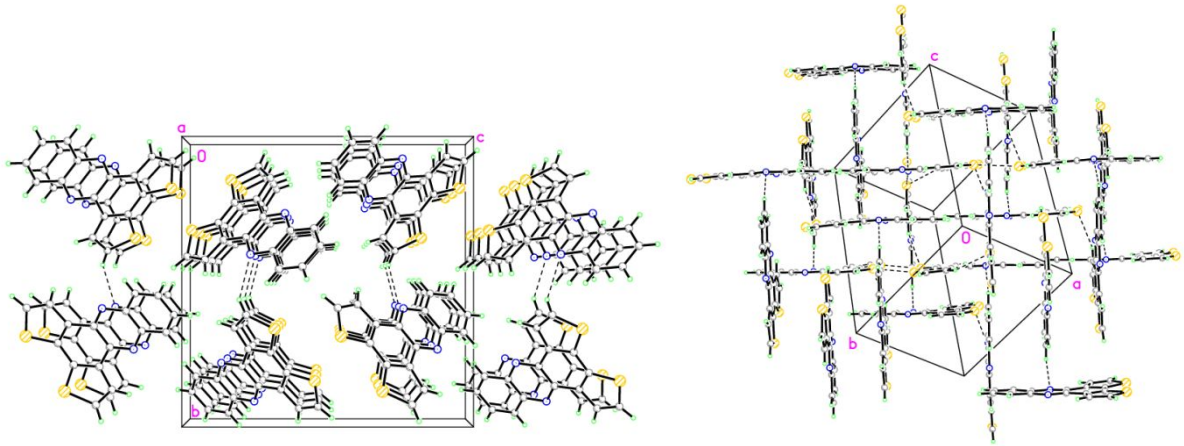

(a) **(b)**

Figure 1. The crystal packing in **α H–DTPhz** (a) and **β H–DTPhz** (b). This and all following figures were prepared using XP program.[49]

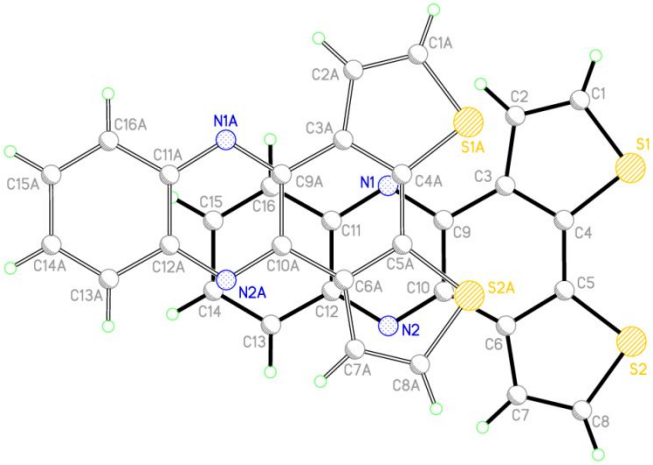

Figure 2. An overlay scheme of the molecules in stacks of **α H–DTPhz**. The symmetrically equivalent atoms are denoted with suffix A.

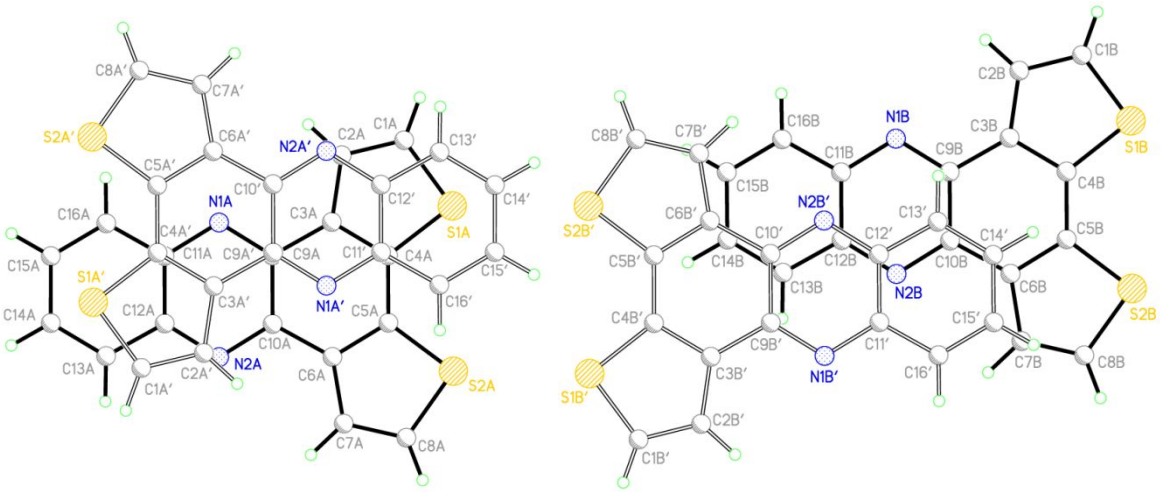

(a) **(b)**

Figure 3. An overlay scheme of the antiparallel molecules **A** (a) and **B** (b) in dimers of **β H–DTPhz**. The symmetrically equivalent atoms are denoted with prime.

Crystallization of **F-DTPhz** from two solvents and vapor phase produced three crystalline forms of this compound. Since substitution of two hydrogen atoms in **H-DTPhz** molecule with two F atoms did not change significantly molecular shape and volume, it was reasonable to suggest that structures of F-substituted phenazines would be isomorphic or at least similar to crystal

structures of unsubstituted molecules. However, structural similarities were not observed for these derivatives, on the contrary, it appeared that F-substituted compound was quite unique, demonstrating packing in crystals with several systems of symmetrically independent molecules and significant impact of specific F···F, C···F, and CH···F interactions in the crystal packing (Tables S1, S2, Figs S6, S8, S10).[65-68]

The crystal packing in the triclinic polymorph **α F-DTPhz** is very uncommon; its asymmetric unit contains six independent molecules (Figure 4a). Four molecules, **A**, **B**, **E**, and **F** are almost parallel, with the interplanar angles between plane of molecule **A** and molecules **B**, **E**, **F** equal to 4.1, 3.6, 3.6°, respectively. These molecules are arranged in stacks along the [1 0 0] direction. The distances between the molecular centroids and the planes of neighboring molecules in stack vary from 3.3 to 3.5 Å. The two other molecules, **C** and **D**, are almost orthogonal to the previous four (for instance, **C**/**A** and **D**/**A** angles are equal to 93.6 and 92.6°), and form a dimer. The angle between molecular planes in **CD** dimer is 9.3°. The distance from the centroid of molecule **C** to the plane of molecule **D** is 3.4 Å. From specific interactions the most meaningful contacts are F(2D)···F(1B) 2.744(3) Å, F(2)···N(1C) 2.874 Å, S(2B)···S(2B)=3.204(1) Å, S(2A)···S(2A) 3.513 Å, and numerous CH···F contacts (Table S1).

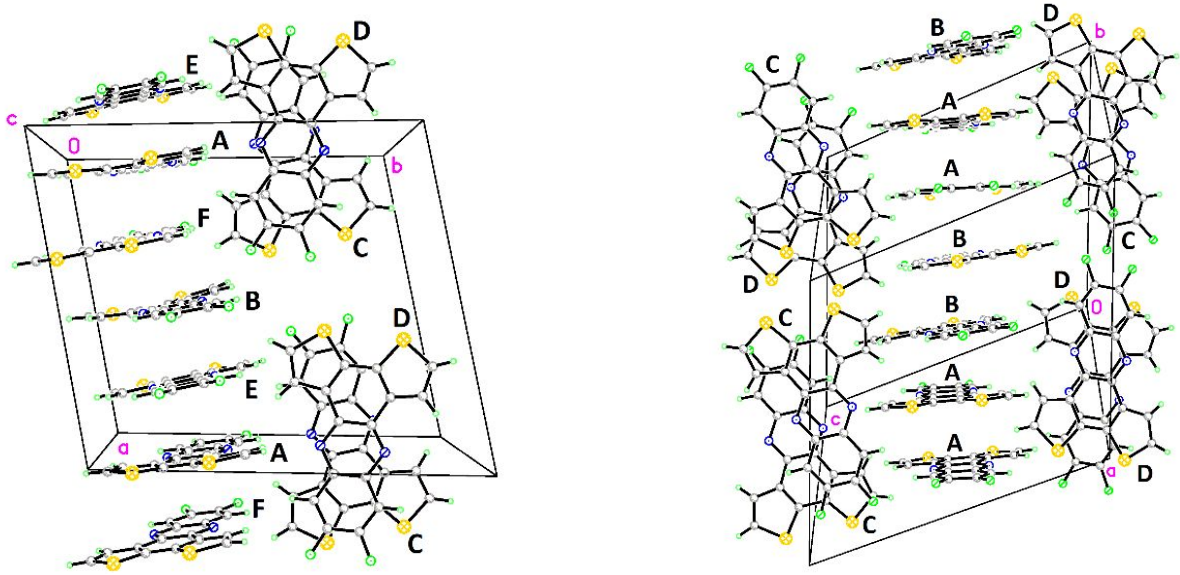

(a) **(b)**

Figure 4. An arrangement of the symmetrically independent molecules in crystal structures of **α F-DTPhz** (a) and **β F-DTPhz** (b).

The crystal of triclinic polymorph **β F-DTPhz**, obtained from vapor phase, contains four symmetrically independent molecules, **A**, **B**, **C**, and **D** (Figure 4b). Molecules are arranged into dimers **AB** and **CD** (Figure 5), which are stacked along the [0 1 0] and [1 1 0] directions, respectively. The interplanar angles are 4.2° and 4.1° in dimers **AB** and **CD**. In both dimers the distances from the centroid of one molecule to the plane of the second molecule are in the range of 3.4 – 3.5 Å. The molecules from different dimers are situated in approximately perpendicular positions, but to a lesser extent than in **α F-DTPhz** polymorph. The interplanar angles between molecules from different dimers range from 76.8 to 81.5°. The molecular arrangement in the crystal is somewhat similar to the arrangement in **α F-DTPhz** crystal (Figure 4), however, in structure of **α F-DTPhz**, dimers **CD** do not form infinite stacks, but associate in tetramers via edge-to edge contact, F(2)···S(3) 3.093(2) Å. The set of intermolecular interactions is poorer than in **α**-polymorph (Table S1) and does not contain F···F short contacts.

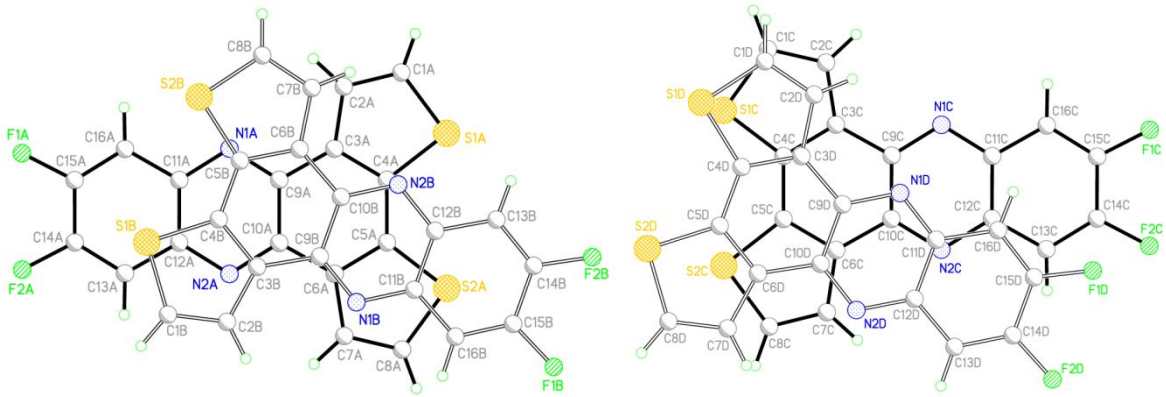

Figure 5. The overlay schemes of molecules **A** and **B** with antiparallel (a) and **C** and **D** with parallel molecular organization (b) in **β F-DTPhz**.

The third **γ F-DTPhz** polymorph (Figure 6) crystallizes in the monoclinic *C*2/*c* group and contains only one molecule in the asymmetric unit. Similar to **α H-DTPhz** polymorph, the molecules form translational stacks along the shortest *b*-axis (Table 1) with interplanar distance of 3.39 Å (Figure 7). In both cases the stacks progress along the shortest axes, *b* in **γ F-DTPhz** and *a* in **α H-DTPhz**, that tells about similarity of stacks in these two forms. The interplanar angle between molecules from neighboring stacks is 89.9°. Analogously to **α H-DTPhz** and **β F-DTPhz**, molecules form planar S…S connected dimers with S…S distances 3.488(2) and 3.577(2) Å. Centrosymmetric dimers are associated in the planar tapes via centrosymmetric weak contacts

H(3)…F(1) 2.63 Å, and form the stacking walls. No other short edge-to-edge intermolecular interactions were found between stacking walls related by the two-fold screw axis.

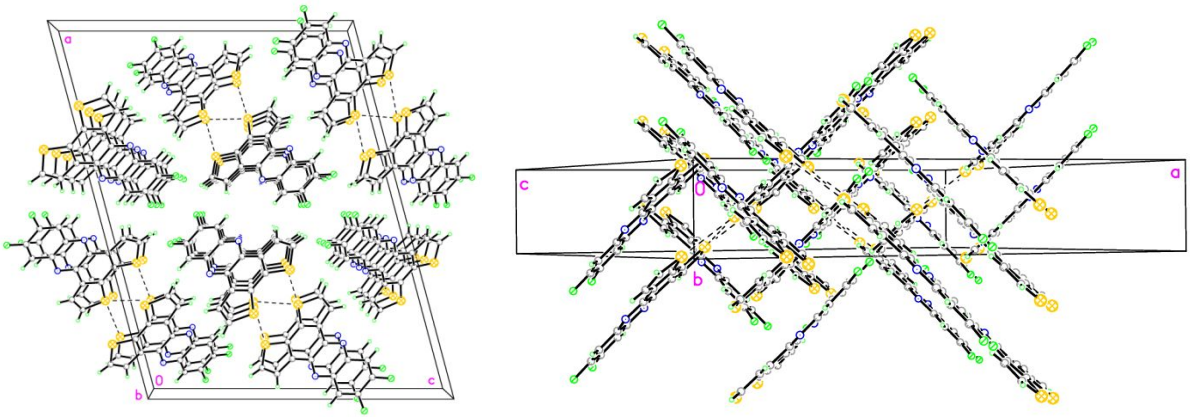

Figure 6. Crystal packing of **γ F-DTPhz** in two orientations.

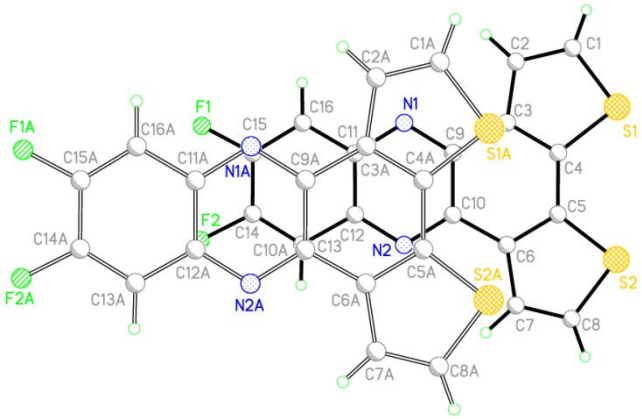

Figure 7. An overlay scheme of the molecules in stacks in **γ F–DTPhz**. The symmetrically equivalent atoms are denoted with suffix A.

The monoclinic **α Cl-DTPhz** contains molecular stacks along the [1 0 0] direction (Figure 8a). The distance between molecular planes is 3.41 Å (Figure 9a). Between the neighboring stacks specific C(4)…Cl(2) 3.365(2) Å (Table S1) contacts were registered. The neighboring stacks pack in a herringbone mode, with the interplanar angle of 87.9 ° between adjacent molecules.

In the orthorhombic **β Cl-DTPhz** (Figure 8b), the two independent molecules (**A** and **B**) form dimers (Figure 9b) with interplanar angle equal to 5.0°. The average distance from the centroid of one molecule to the plane of the second one is 3.25 Å. The dimers are arranged in stacks along the [1 0 0] direction. The interplanar distance between neighboring dimers in stacks is larger than

between dimers inside the stack (average centroid–plane distance is 3.45 Å), and the overlapping area is smaller.

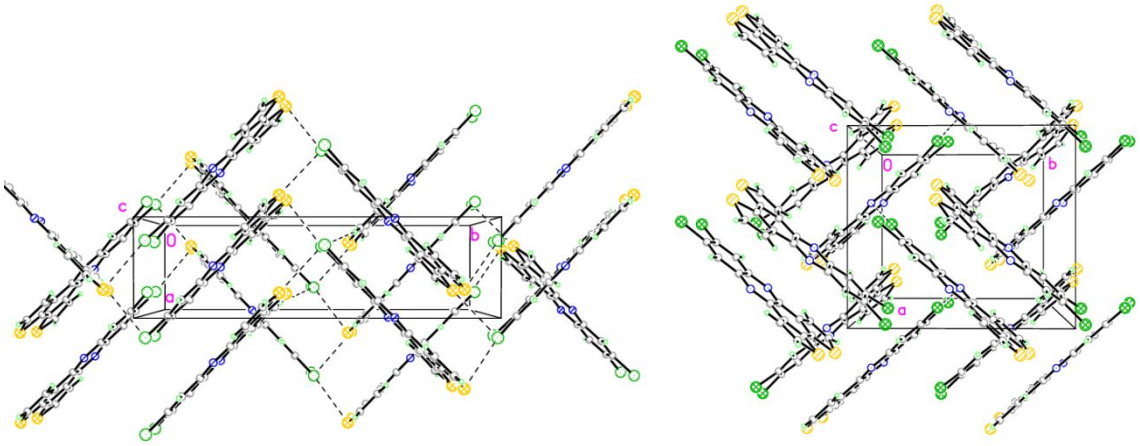

(a) **(b)**

Figure 8. The crystal structures of **α Cl-DTPhz** (a) and **β Cl-DTPhz** (b).

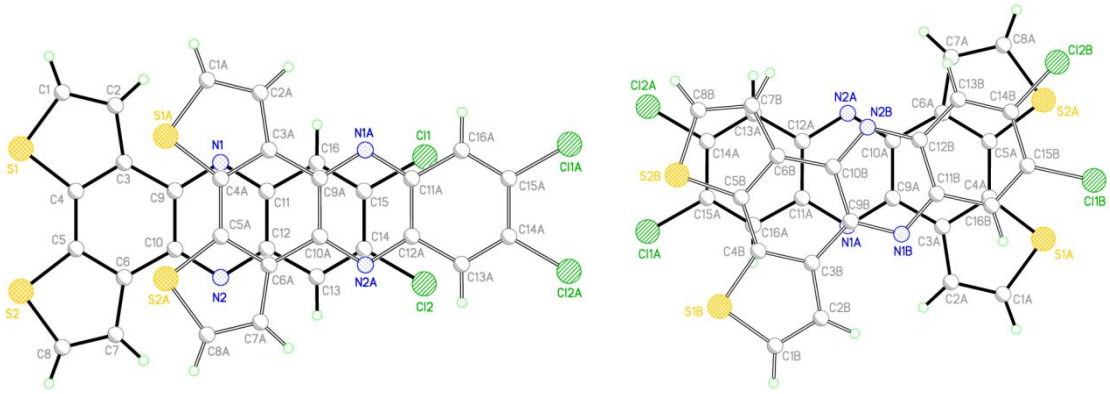

(a) **(b)**

Figure 9. An overlay scheme of the parallel molecules in **α Cl-DTPhz** (a) and antiparallel in **β Cl-DTPhz** (b).

The crystal structure of **Br-DTPhz** is isomorphic to the **β Cl-DTPhz**. The interplanar angle in dimers is 4.5°. The distance from the centroid of one molecule to the plane of the second molecule is 3.28 Å. The interplanar distance between neighboring dimers in stack is larger than inside the stack (centroid –plane distance is 3.43 Å).

In **TMS-F-DTPhz** that crystallizes in the orthorhombic *Pnma* space group (Table 2), molecules occupy special positions on the mirror plane. The molecules form stacks along the [0 1 0] direction. The distance between planes of molecules in stacks is 3.48 Å. The crystal structure of **TMS-Cl-DTPhz** also consists of stacked molecules. The distances between planes of molecules

in the stacks are 3.44 and 3.46 Å. In both structures, molecules pack in an antiparallel mode (Figure 10), most favorable in the presence of bulky TMS substituents.

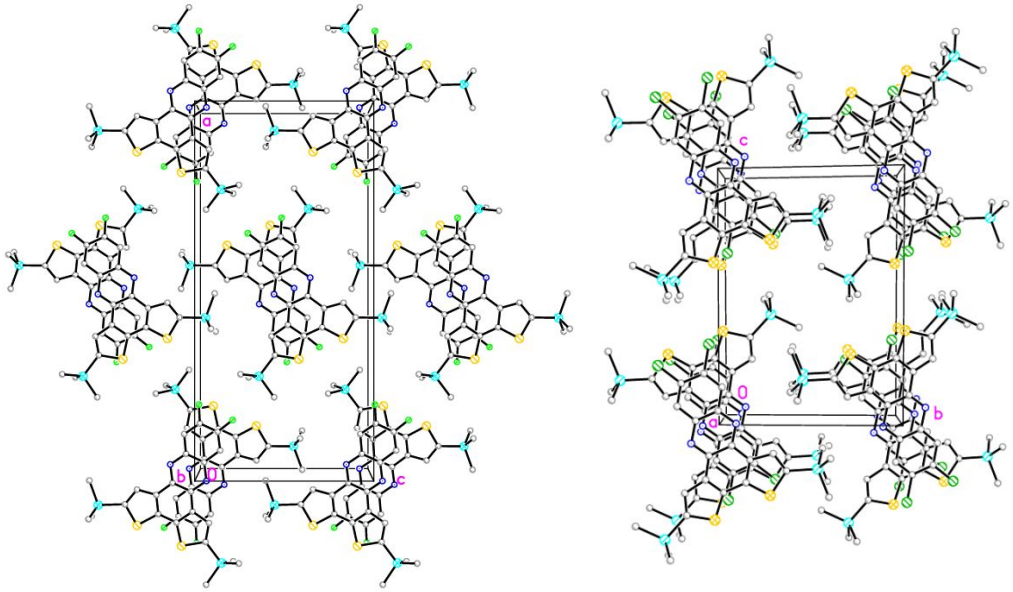

(a) **(b)**

Figure 10. Packing in the crystal structures of **TMS-F-DTPhz** (a) and **TMS-Cl-DTPhz** (b) demonstrating molecular stacks with antiparallel arrangement of molecules in both crystals.

In the reported compounds, the interplanar distances in the stacking dimers range from 3.25 to 3.53 Å, that is consistent with values for analogous compounds, where such distances range from 3.25 to 3.61 Å.[69, 70]

The size and shape of Hirshfeld surfaces (HS) help identify intermolecular interactions and classify molecular crystals in terms of packing similarities. The CrystalExplorer program[55] was used to generate Hirshfeld surfaces and fingerprint plots in eight **R-DTPhz** (R=H, F, Cl, Br) compounds taking in consideration in all cases the contents of the asymmetric units. The main contributions to the total HS areas were depicted by the d_{norm} surfaces (Figures S1, S3, S5, S7, S9, S11, S13, S15) and by the full and decomposed fingerprint plots (Figures S2, S4, S6, S8, S10, S12, S14, S16 in Supporting Information file) and numerical values were summarized in Table S2. It was evident, that in the lack of strong donor centers in the molecules all the registered interactions were concentrated in the area of weak interactions with the predominant impact of those with H-participation, like H···H, and H···X(X= N, C, S, F, Cl, Br). Particularly H···H interactions

comprised 35.7 and 34.6% in **H-DTPhz** polymorphs, with the decreasing of this value up to 18.8-23.0 % in the halogen-substituted compounds (Table S2) in favor of impact of H···Hal interactions that varied in the range 10.8% (**α Cl-DTPhz**) -19.3% (**Br-DTPhz**). The C···C contacts associated with π-π stacking interactions were registered with the meaningful contributions, 7.5% (**Br-DTPhz**) – 15.0% (**α F-DTPhz**) in all compounds.

Computational analysis. The quantum chemical calculations showed that substituents at positions 9 and 10 in a series of **H-DTPhz, F-DTPhz**, and **Cl-DTPhz** do not have significant effect on HOMO and LUMO wave functions, and both frontier orbitals are delocalized over whole π-system (Figure 11). The electron density on halogen atoms **F-DTPhz**, **Cl-DTPhz** and **Br-DTPhz** is present in both HOMO and LUMO with stabilization of both frontier orbitals by approximately 0.2 eV in comparison with unsubstituted **H-DTPhz**, resulting in similar HOMO-LUMO gaps (Table 3). In addition, the first excitation energies for all molecules were calculated with TD-DFT method (Table 3).

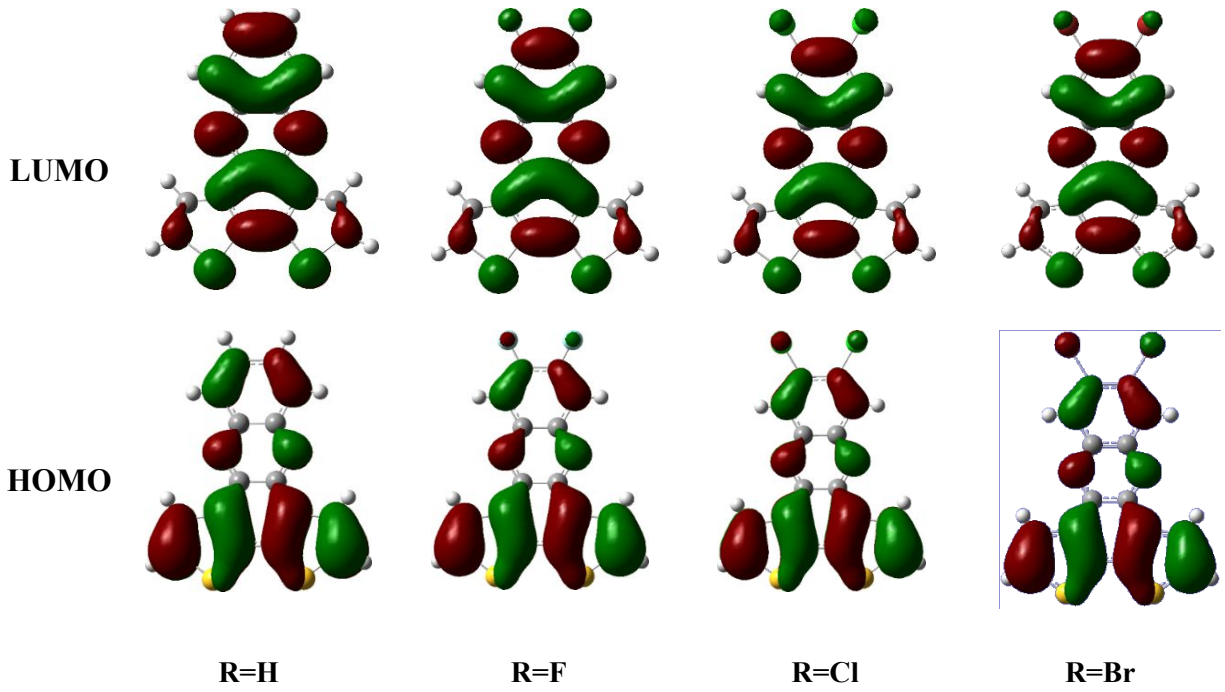

Figure 11. Pictorial representations of the HOMO and LUMO wave functions of **R-DTPhz** (**R=H, F, Cl, Br**) as determined at the B3LYP/6-311G(d) level of theory.

Table 3. Theoretical calculations of orbital energies in DTPhz derivatives (eV)

	H-DTPhz	**F-DTPhz**	**Cl-DTPhz**	**Br-DTPhz**	**F-TMS-DTPhz**	**Cl-TMS-DTPhz**
	B3LYP/6-311G(d)					
E_{HOMO}	-5.93	-6.10	-6.16	-6.14	-5.96	-6.01
E_{LUMO}	-2.56	-2.78	-2.92	-2.91	-2.70	-2.84
E_{gap}	3.37	3.32	3.34	3.23	3.26	3.17
TD-DFT	2.85	2.79	2.71	2.70	2.73	2.64
	M06/6-311G(d)					
E_{HOMO}	-6.20	-6.37	-6.41	-6.39	-6.23	-6.28
E_{LUMO}	-2.40	-2.62	-2.75	-2.73	-2.55	-2.68
E_{gap}	3.79	3.75	3.66	3.66	3.68	3.60
TD-DFT	2.95	2.90	2.82	2.82	2.84	2.76

The calculated TD-DFT energy for **H-DTPhz** is almost the same as electrochemical band gap 2.87 eV.[40] It should be mentioned that cyclic voltammetry analysis presented there in demonstrated that TMS groups have only marginal impact on both half-wave reduction potentials of **H-TMS-DTPhz** (–1.80 V and –1.79 V, for **H-TMS-DTPhz** and **H-DTPhz** respectively) and oxidation potentials (+1.06 and + 1.08 V, respectively) with their difference for **H-DTPhz** equal 2.87 V and for **H-TMS-DTPhz** 2.86 V. These results also agree with computational data presented in Table 3.

Crystal energy calculations of polymorphs

Results of X-ray studies demonstrated that **DTPhz** derivatives crystallize in seven different crystal packing types, I-VII, which correspond to experimental crystal structures of **α H-DTPhz**, **β H-DTPhz**, **α F-DTPhz**, **β F-DTPhz**, **γ F-DTPhz**, **α Cl-DTPhz**, and **β Cl-DTPhz** (which is also isomorphous to **Br-DTPhz**). To evaluate if all these packing types have some probability of realization for all four **DTPhz** derivatives (R=H, F, Cl, Br), lattice energy computations of these seven types for each R substituent were carried out with quantum-chemistry periodic plane-wave DFT and empirical force field methods (Table 4). In the case of experimental polymorphs, the X-ray crystal structures were used as initial models with C–H bonds normalized to standard distance 1.09 Å. For the hypothetical structures, the halogen or hydrogen atoms of the experimental polymorph were substituted with R atoms of the corresponding **R-DTPhz** derivative. For example, for energy calculation of the polymorph of **F-DTPhz** with the crystal structure VI (**α Cl-DTPhz**),

Cl atoms in **α Cl-DTPhz** were substituted with F atoms. For all calculated structures, the optimization of atomic coordinates and unit cell parameters was carried out.

The results of quantum-chemical (PBE-D method) and force field (COMAPSS Force Field) calculations of relative energies for experimentally observed and hypothetical polymorphs are presented in Table 4; the energies that correspond to the experimentally found structures are presented in bold font. For both methods, the low-lying polymorphs correspond to experimentally observed structures. The quantum-chemical calculations demonstrated a polymorphic diversity of **F-DTPhz** compound, which is in agreement with experimental data. The calculated relative energies in PBE-D method show that **F-DTPhz** has a high probability to crystallize in six of seven crystalline forms. Such behavior can be explained by geometrical and electronic properties of **F-DTPhz** molecule. Geometrically, it is similar to **H-DTPhz** molecule, since C–F bond distances (1.35 Å) are not much longer that C–H bond distances (1.09 Å), and at the same time its dipole moment (2.65 D) is close to dipole moments of **Cl-DTPhz** (3.12 D) and **Br-DTPhz** (2.71 D). The relative energies for **H-DTPhz** show that, in addition to experimentally observed polymorphs **α** and **β** (I and II polymorph type), it can also form three polymorphs with crystal packing of types IV–VI (structures of **β F-DTPhz**, **γ F-DTPhz**, and **α Cl-DTPhz**). The experimentally observed **Cl-DTPhz** polymorphs (structures VI and VII) are more than 2.0 kcal/mol lower in energy than hypothetical polymorphs. This can be explained by the geometrical factor because the C–Cl distance, 1.72 Å, is much longer than C–H and C–F distances. For the **Br-DTPhz**, for which only one polymorph VII was experimentally observed, PBE-D calculations suggest the second possible polymorph corresponding to structure of **α Cl-DTPhz**; both modeled structures VI and VII for **Br-DTPhz** have the same energies. This can be explained by the geometrical (C–Br distance is 1.89 Å) and electronic similarities of both molecules.

Table 4. The relative energies (kcal/mol) for seven types of polymorphs of R-DTPhz derivatives

polymorph	I	II	III	IV	V	VI	VII
structure type	**α H-DTPhz**	**β H-DTPhz**	**α F-DTPhz**	**β F-DTPhz**	**γ F-DTPhz**	**α Cl-DTPhz**	**β Cl-DTPhz**
	PBE-D						
H	**0.0**	**0.9**	4.9	1.7	1.7	1.4	5.3
F	0.1	2.7	**0.3**	**0.0**	**0.0**	0.1	0.3
Cl	3.6	8.1	3.8	2.4	2.8	**0.1**	**0.0**

Br						0.0	**0.0**
	COMPASS Force Field						
H	**0.9**	**0.6**	3.4	0.5	**0.0**	0.2	4.7
F	2.2	4.4	**3.3**	**1.2**	**0.0**	1.4	4.3
Cl	3.0	4.8	2.9	2.3	2.6	**0.0**	**1.3**
Br	3.4	5.4	3.0	2.7	3.6	0.0	**0.7**

The COMPASS Force Field calculations show similar energy ranging for the polymorphs of **H-DTPhz**, **Cl-DTPhz**, and **Br-DTPhz**. For **H-DTPhz** compound, the calculations also predict possibility of polymorphs IV–VI. For the molecules of **Cl-DTPhz** and **Br-DTPhz**, only structures VI and VII correspond to low-lying polymorphs. For the **F-DTPhz** compound, COMPASS Force Field also predicts additional polymorphs, however the calculated lattice energy for α **F-DTPhz** is 3.3 kcal/mol higher than for **γ F-DTPhz**, and thus α **F-DTPhz** should be unstable. Such deficiency of calculations can be caused by the presence of six symmetrically independent molecules that significantly increases the number of variable parameters and complicates optimization.

4. CONCLUSIONS

Several new materials including dithieno[3,2-*a*:2',3'-*c*]phenazine and its 9,10-dihalogen derivatives (Hal=F, Cl, Br) with general formula **R-DTPhz** have been characterized with experimental and computational methods. Crystals for X-ray diffraction analysis were prepared using solutions and gas phase crystal growth methods, with and without TCNQ conformer, which lead to formation of seven packing polymorphs for three compounds with R=H, F and Cl. In spite of similar molecular structure, all seven packing patterns are rather different, including two very uncommon crystal structures with 6 and 4 symmetrically independent molecules per asymmetric part of the unit cell (R=F). Results of quantum chemical calculations of lattice energy for H-, F- and Cl-substituted **R-DTPhz** polymorphs demonstrate that the low-lying polymorphs correspond to the experimentally observed structures. In all studied compounds π-stacked associates (dimers or stacks) with molecular interplanar distances below 3.5 Å were found that indicates, along with the voltametric and computational data on HOMO-LUMO band gaps, that they might be useful for formation of two-component co-crystals with stacked structure for potential applications in organic electronics. The most probable candidate to be employed in organic electronics seems us **γ F-DTPhz** which structure and crystal shape are similar to characteristics found for **α F-DTPhz,** which is described in the literature as crystalline elastic waveguide.[41]

It should be mentioned that for compounds **Br-DTPhz**, **TMS-F-DTPhz** and **TMS-Cl-DTPhz,** only one polymorph was found experimentally, however energy calculations of series of crystal structures of these materials demonstrated high probability of finding several more polymorphs for these compounds.

Author Contributions

Conceptualization, B.B.A., T.V.T.; methodology, B.B.A.; investigation, B.B.A., R.C., E.V.J.; writing—original draft preparation, B.B.A., M.S.F., T.V.T.; writing—review and editing, all authors; visualization, all authors; funding acquisition, T.V.T.; All authors have read and agreed to the published version of the manuscript.

Conflicts of Interest

The authors declare no conflict of interest.

Acknowledgments

We thank Y. Getmanenko for supplying us with materials which she synthesized during her employment as a postdoc at NMHU. We are grateful for Hui Jiang and Christian Kloc for assistance with crystal growth by PVT method. The authors also gratefully acknowledge the Ohio Supercomputer Center for providing computational resources. This work had been supported by NSF via DMR-1523611 and DMR-2122108 (PREM). M.S.F. thanks the project ANCD 20.80009.5007.15 for support

REFERENCES

1. W. C. McCrone, In Physics and Chemistry of the Organic Solid State; D. Fox, M. Labes, A. Weissenberg, Eds.; Interscience Publishers: New York: 1965; Vol. 2, p 725.
2. J. Bernstein, Polymorphism in Molecular Crystals; Oxford University Press, Oxford, 2002.
3. In Crystal Engineering: The Design and Application of Functional Solids; K. R. Seddon, M. Zaworotko, Eds.; Kluwer Academic: 1999; Vol. 539.
4. G. M. Day, A. V. Trask, W. D. S. Motherwell and W. Jones, *Chem. Comm*., 2006, 54-56.
5. F. J.J. Leusen, and J. Kendrick, Polymorph Prediction of Small Organic Molecules, Co-crystals and Salts In: Pharmaceutical Salts and Co-crystals, Johan Wouters, editor, Royal Soc. of Chemistry, 2011. Chapter 4, 44-88.
6. C. Bodewig, *Zeitschrift für Kristallographie - Crystalline materials*. 1881, **5**, 554-576.
7. P. K. Thallapally, R. K. R. Jetti, A. K. Katz, H. L. Carrell, K. Singh, K. Lahiri, S. Kotha, R. Boese and G. R. Desiraju, *Angew. Chem. Int. Ed*. 2004, **43**, 1149-1155.

8. T. V. Timofeeva, G. H. Kuhn, V. V. Nesterov, V. N. Nesterov, D. O. Frazier, B. G. Penn, and M. Y. Antipin, *Cryst. Growth Des.* 2003, **3**, 383-391.
9. R. Castañeda, S. A. Antal, S. Draguta, T. V. Timofeeva, V. N. Khrustalev, *Acta Crystallogr. Section E: Structure Reports Online.* 2014, **70**, o924-o925.
10. E. H. Lee, *Asian J. Pharm. Sci.* 2014, **9**, 163-175.
11. R.-Q. Song, and H. Colfen, *CrystEngComm* 2011, **13**, 1249-1276.
12. G. Mehta, S. Sen, and K. Venkatesan, *CrystEngComm* 2007, **9**, 144-151.
13. G. Cavallo, P. Metrangolo, R. Milani, T. Pilati, A. Priimagi, G. Resnati and G. Terraneo, *Chem. Rev.,* 2016, **116**, 2478–2601.
14. S. K. Seth, P. Manna, N. J. Singh, M. Mitra, A. D. Jana, A. Das, S. R. Choudhury, T. Kar, S. Mukhopadhyay and K. S. Kim, *CrystEngComm***,** 2013,**15**, 1285-1288.
15. K. Bechgaard, T. J. Kistenmacher, A. N. Bloch and D. O. Cowan, *Acta Crystallogr. Sect. B,* 1977, **33**, 417-422.
16. T. J. Kistenmacher, T. J. Emge, A. N. Bloch and D. O. Cowan, *Acta Crystallogr. Sect. B,* 1982, **38**, 1193-1199.
17. M. Courté, J. Ye, H. Jiang, R. Ganguly, S. Tang, C. Kloc and D. Fichou, *Phys. Chem. Chem. Phys.,* 2020, **22**, 19855-19863.
18. D. Gentili, M. Gazzano, M. Melucci, D. Jones and M. Cavallini, *Chem. Soc. Rev.*, 2019,**48**, 2502-2517.
19. S. Yan, A. Cazorla, A. Babuji, E. Solano, C. Ruzié, Y. H. Geerts, C. Ocal and E. Barrena, *Phys. Chem. Chem. Phys.*, 2022, **24**, 24562.
20. R. Bhowal and D. Chopra, *Cryst. Growth Des.,* 2021, 21, 4162−4177.
21. M. L. Tang and Z. A. Bao, *Chem. Mater.,* 2011, **23**, 446-455.
22. H. Chung and Y. Diao, *J. Mater. Chem., C* 2016, **4**, 3915-3933.
23. Y.-G. Zhen, H.-L. Dong, L Jiang and W.-P. Hu, *Chinese Chem. Lett.,* 2016, **27**, 1330-1338.
24. O. D. Jurchescu, D. A. Mourey, S. Subramanian, S. R. Parkin, B. M. Vogel, J. E. Anthony, T. N. Jackson and D. J. Gundlach, *Phys. Rev. B* 2009, **80**, 085201.
25. L. A. Stevens, K. P. Goetz, A. Fonari, Y. Shu, R. M. Williamson, J.-L. Brédas, V. Coropceanu, O. D. Jurchescu and G. E. Collis, *Chem. Mater.*, 2015, **27**, 112-118.
26. J. A. Schneider, H. Black, H.-P. Lin and D. F. Perepichka, *ChemPhysChem,* 2015, **16**, 1173-1178.

27. Q. Guo, L. Wang, F. Bai, Y. Jiang, J. Guo, B. Xu and W. Tian, *RSC Adv.,* 2015, **5**, 18875-18880.
28. G. Wesela-Bauman, S. Lulinski, J. Serwatowski and K. Wozniak, *Phys. Chem. Chem. Phys*., 2014, **16**, 22762-22774.
29. H.-Z. Gao, *Int. J. Quantum Chem.,* 2012, **112**, 740-746.
30. F. Yu, G. Yang and Z. Su, *Synth. Met*., 2011, **161**, 1073-1078.
31. W. Ratzke, L. Schmitt, H, Matsuoka, C. Bannwarth, M. Retegan, S. Bange, P. Klemm, F. Neese, S. Grimme, O. Schiemann, J. M. Lupton and S. Hoeger, *J. Phys. Chem. Lett*., 2016, **7**, 4802-4808.
32. J. Z. Fan, Y. Zhang, C. L Lang, M. Qiu, J. S. Song, R. Q. Yang, F. Y. Guo, Q. J. Yu, J. Z. Wang and L. C. Zhao, *Polymer*, 2016, **82**, 228-237.
33. Y. Zhang, J. Y Zou, H. L. Yip, K. S. Chen, J. A. Davies, Y. Sun and A. K. Y. Jen, *Macromolecules,* 2011, **44**, 4752-4758.
34. M. L. Keshtov, S. A. Kuklin, N. A. Radychev, A. Y. Nikolaev, I. E. Ostapov, M. M. Krayushkin, I. O. Konstantinov, E. N. Koukaras, A. Sharmag and G. D. Sharma, *Phys. Chem. Chem. Phys*., 2016, **18**, 8389-8400.
35. C. A. Richard, Z. X. Pan, H. Y. Hsu, S. Cekli, K. S. Schanze and J. R. Reynolds, *ACS Appl. Mater. Inter.,* 2014, **6**, 5221-5227.
36. C. A. Richard, Z. Pan, A. Parthasarathy, F. A. Arroyave, L. A. Estrada, K. S. Schanze and J. R. Reynolds, *J. Mater. Chem. A,* 2014, **2**, 9866-9874.
37. X. Lu, T. Lan, Z. Qin, Z.-S. Wang and G. Zhou, *ACS Appl. Mater. Interfaces,* 2014, **6**, 19308-19317.
38. T. H. El-Assaad, S. B. Shiring, Y. A. Getmanenko, K. M. Hallal, J. L. Bredas, S. R. Marder, M. H. Al-Sayah and B. R. Kaafarani, *RSC Adv,* 2015, **5**, 43303-43311.
39. D. Yokoyama, H. Sasabe, Y. Furukawa, C. Adachi and J. Kido, *Adv. Funct. Mat*., 2011, **21**, 1375-1382.
40. Q. Ai, Y.A. Getmanenko, K. Jarolimek, R. Castañeda, T.V. Timofeeva and C. Risko, *J. Phys. Chem. Lett*., 2017, **8**, 4510-4515.
41. M. Annadhasan, A.R. Agrawal, S. Bhunia, V.V. Pradeep, S.S. Zade, C.M. Reddy and R. Chandrasekar, *Angew. Chem., Int. Ed.,* 2020, **59**, 13852-13858.
42. X. Song, H. Yu, Y. Zhang, Y. Miao, K. Ye and Y. Wang, *CrystEngComm*, 2018, **20**,1669-1678.
43. X. Song, Z. Zhang, S. Zhang, J. Wei, K. Ye, Y. Liu, T.B. Marder, and Y. Wang, *J. Phys. Chem. Lett.* 2017, **8**, 3711-3717.

44. P. Brooks, D. Donati, A. Pelter, and F. Poticelli, *Synthesis,* 1999, **1999**, 1303-1305.
45. Y. A. Getmanenko, C. Risko, P. Tongwa, E. G. Kim, H. Li, B. Sandhu, T. Timofeeva, J. L. Bredas and S. R. Marder, *J. Org. Chem*. 2011, **76**, 2660-2671.
46. Y. A. Getmanenko, P. Tongwa, T. V. Timofeeva and S. R. Marder, *Org. Lett.* 2010, **12**, 2136-2139.
47. Y. A. Getmanenko, M. Fonari, C. Risko, B. Sandhu, E. Galan, L. Y. Zhu, P. Tongwa, D. K. Hwang, S. Singh, H. Wang, S. P. Tiwari, Y. L. Loo, J. L. Bredas, B. Kippelen, T. Timofeeva and S. R. Marder, *J. Mater. Chem*. *C*, 2013, **1**, 1467-1481.
48. R. A. Laudise, C. Kloc, P. G. Simpkins and T. Siegrist, *J. Cryst. Growth,* 1998, **187**, 449-454.
49. Bruker-AXS; 2.2012.2 0 ed.; Bruker AXS: Madison, Wisconsin, USA, 2009.
50. Bruker-AXS; 2014.11-0 ed.; Bruker AXS: Madison, Wisconsin, USA, 2014.
51. G. M. Sheldrick, 2012/1 ed. University of Göttingen, Göttingen, Germany 2012.
52. G. M. Sheldrick*, Acta Cryst. Sect.* A: **2008**, **A64**, 112-122.
53. G. M. Sheldrick, *Acta Crystallogr., Sect. A: Found. Adv*. **2015**, **A71**, 3-8.
54. C. F. Macrae, I. J. Bruno, J. A. Chisholm, P. R. Edgington, P. McCabe, E. Pidcock, L. Rodriguez-Monge, R. Taylor, J. van de Streek and P. A. Wood, *J. Appl. Crystallogr.,* 2008, **41,** 466-470.
55. P. R. Spackman, M. J. Turner, J. J. McKinnon, S. K. Wolff, D. J. Grimwood, D. Jayatilaka and M. A. Spackman, CrystalExplorer: a program for Hirshfeld surface analysis, visualization and quantitative analysis of molecular crystals. *J. Appl. Crystallogr.,* 2021, **54**, 1006–1011.
56. M. J. Frisch, G. W. Trucks, H. B. Schlegel, G. E. Scuseria, M. A. Robb, J. R. Cheeseman, G. Scalmani, V. Barone, G. A. Petersson, H. Nakatsuji, X. Li, M. Caricato, A. Marenich, J. Bloino, B. G. Janesko, R. Gomperts, B. Mennucci, H. P. Hratchian, J. V. Ortiz, A. F. Izmaylov, J. L. Sonnenberg, D. Williams-Young, F. Ding, F. Lipparini, F. Egidi, J. Goings, B. Peng, A. Petrone, T. Henderson, D. Ranasinghe, V. G. Zakrzewski, J. Gao, N. Rega, G. Zheng, W. Liang, M. Hada, M. Ehara, K. Toyota, R. Fukuda, J. Hasegawa, M. Ishida, T. Nakajima, Y. Honda, O. Kitao, H. Nakai, T. Vreven, K. Throssell, J. A. Montgomery, Jr., J. E. Peralta, F. Ogliaro, M. Bearpark, J. J. Heyd, E. Brothers, K. N. Kudin, V. N. Staroverov, T. Keith, R. Kobayashi, J. Normand, K. Raghavachari, A. Rendell, J. C. Burant, S. S. Iyengar, J. Tomasi, M. Cossi, J. M. Millam, M. Klene, C. Adamo, R. Cammi, J. W. Ochterski, R. L. Martin,

K. Morokuma, O. Farkas, J. B. Foresman and D. J. Fox, Gaussian, Inc.: Wallingford, CT, USA, 2009

57. H. Sun, COMPASS: *J. Phys. Chem*. B 1998, **102**, 7338-7464.
58. P. Verwer and F. J. J. Leusen, Computer Simulation to Predict Possible Crystal Polymorphs. In: Reviews in Computational Chemistry; John Wiley & Sons, Inc.: 2007, p 327.
59. A. M.; Rappe, K. M.; Rabe, E.; Kaxiras and J. D. Joannopoulos, *Phys. Rev*. B 1990, **41**, 1227-1230.
60. S. Grimme, *J. Comp. Chem*. 2006, **27**, 1787-1799.
61. V. Barone, M. Casarin, D. Forrer, M. Pavone, M.Sambi and A. Vittadini, *J. Comp. Chem*. 2009, **30**, 934-939.
62. P. Giannozzi, S. Baroni, N. Bonini, M. Calandra, R. Car, C. Cavazzoni, D. Ceresoli, G. L. Chiarotti, M. Cococcioni, I. Dabo, A. Dal Corso, S. Fabris, G. Fratesi, S. de Gironcoli, R. Gebauer, U. Gerstmann, C. Gougoussis, A. Kokalj, M. Lazzeri, L. Martin-Samos, N. Marzari, F. Mauri, R. Mazzarello, S. Paolini, A. Pasquarello, L. Paulatto, C. Sbraccia, S. Scandolo, G. Sclauzero, A. P. Seitsonen, A. Smogunov, P. Umari and R. M. Wentzcovitch, QUANTUM ESPRESSO: a modular and open-source software project for quantum simulations of materials. *J. Phys.Condens Matter.* 2009, **21**, 395502.
63. C. R. Groom, I. J. Bruno, M. P. Lightfoot and S. C. Ward, *Acta Crystallogr. Sect*. B, 2016, **72**, 171-179.
64. C. F. Matta, J. Hernández-Trujillo, T.-H. Tang and R. F. W. Bader, *Chem. Eur. J.* 2003, **9**, 1940-1951.
65. V. R. Hathwar and T. N. Guru Row, *Cryst. Growth Des.,* 2011, **11**, 1338–1346.
66. V. R. Thalladi, H.-C. Weiss, D. Bla1ser, R. Boese, A. Nangia and G. R. Desiraju, *J. Am. Chem. Soc.*, 1998, **120**, 8702-8710.
67. K. Reichenbächer, H. I. Süss and J. Hulliger, *Chem. Soc. Rev.*, 2005, **34**, 22-30.
68. D. E. Arkhipov, A. V. Lyubeshkin, A. D. Volodin and A. A. Korlyukov, *Crystals*, 2019, **9**, 242.
69. A. Putta, J. D. Mottishaw, Z. Wang and H. Sun, *Cryst. Growth Des*., 2014, **14**, 350-356.

70. M. O. BaniKhaled, J. D. Mottishaw and H. Sun, *Cryst. Growth Des*., 2015, **15**, 2235-2242.